Mechanism for phase transitions and vacancy island formation in alkylthiol/Au(111) self-assembled monolayers based on adatom and vacancy-induced reconstructions

Edmanuel Torres, Alexander T. Blumenau,* and P. Ulrich Biedermann†
Max-Planck-Institut für Eisenforschung GmbH, Max-Planck-Strasse 1, 40237 Düsseldorf, Germany
(Received 6 November 2008; published 26 February 2009)

The structural and energetic effects due to gold adatoms and/or gold surface vacancies in ethylthiol/Au(111) self-assembled monolayers (SAMs) in the high-density regime have been studied. The stability of these SAM structures was evaluated based on adsorption and surface energies that allow a direct comparison of structures with different compositions. We have found another energetically more favorable $c(4\times2)$ structure that includes two adatoms. These adatoms may initially be taken from the gold surface creating vacancies. However our results indicate that the SAM may further stabilize by stepwise filling the surface vacancies. A plausible mechanism for the formation of gold vacancy islands, as seen in experiments during the growth of high-density domains, arises from this stabilization process. The best structure including two adatoms agrees with many structural data derived from the experiments. In particular, the simulated scanning tunneling microscope (STM) image exhibits a zigzag modulation that is characteristic of the δ phase frequently found in STM experiments.

DOI: 10.1103/PhysRevB.79.075440 PACS number(s): 68.43.Fg, 68.43.Hn, 71.15.Mb

I. INTRODUCTION

Self-assembled monolayers (SAMs) have a rapidly growing number of applications in nanotechnology,[1,2] biosciences,[3] and molecular electronics.[4] SAMs are characterized by a spontaneous self-organized formation of highly ordered two-dimensional structures on solid surfaces. Several molecule/surface systems show this fascinating behavior. Many studies have focused on alkylthiol SAMs on Au(111) due to their ease of preparation, high order, and high stability. Furthermore, alkylthiol SAMs on gold are considered as a convenient system to study the intrinsic phenomenon of self-assembly. The surface structures, defects, and dynamics of alkylthiol SAMs on Au(111) were recently reviewed emphasizing the incompleteness of our knowledge.[5]

The formation of alkylthiol/Au(111) SAMs (from solution or gas phase) involves a rapid initial physisorption on the gold substrate followed by slow chemisorption and loss of the mercaptane hydrogen.[5] Self-assembly passes through several low-density phases of different intermediate structures at low coverage and leads to high-density structures with a coverage of 1/3 monolayer. The molecules are strongly bound through the S headgroup and the alkyl chain points upward.[6,7] Simultaneous with the growth of high-density domains, gold vacancy islands are formed, which nucleate outside the ordered domains.[8–10] The size distribution of these pits undergoes an Ostwald ripening due to diffusion of monovacancies.[11] In the final stage, the $(\sqrt{3}\times\sqrt{3})R30°$ structure and several $c(4\times2)$ superlattices coexist[12] in a configuration depending on chain length[13] and surface defects.[14,15] The $c(4\times2)$ phases were first detected during low-temperature infrared measurements[16] and confirmed by several other techniques.[5] Until now six different ordered high-density phases have been reported (see Ref. 17 and references therein). Transformations between these phases have been observed.[14,18,19] The $(\sqrt{3}\times\sqrt{3})R30°$ lattice has sulfur atoms bound on equivalent sites. A combination of molecules adsorbed on inequivalent positions, involving different chain angles, has been proposed for $c(4\times2)$. The atomic structure of the SAMs, in particular, the gold-sulfur binding site and the arrangement of the alkyl chain still remain an open issue.[1,5,20]

Theoretical and experimental studies agree with respect to absorption energies, coverage and periodicity, adsorption via the sulfur headgroup, and upward orientation of the alkyl chain.[21,22] In particular, experimental results and density-functional theory (DFT) calculations agree on the angular orientation of thiols in SAMs, which results from a balance of substrate-molecule and van der Waals interactions.[5] However, concerning the long-standing question of the sulfur adsorption site, diffraction studies have reported the top position as adsorption site.[23,24] More recently, grazing incidence x-ray diffraction (GIXRD) studies confirmed the top site but found good agreement also for fcc and hcp sites. However, the best fit was achieved with a combination of incoherent domains with thiols adsorbed in top and fcc sites.[25] These results contrast with theoretical studies. DFT calculations on unreconstructed Au(111) surfaces predict adsorption on the bridge site, slightly shifted to the fcc hollow, while the top position is very unfavorable.[21,22,26–29] Finding an explanation for the $c(4\times2)$ phases is even more challenging.[22,30] Experiments have shown that a structure with equivalent absorption sites could explain the α phase; however, variations of the twisting angle cannot explain all the $c(4\times2)$ superlattice phases.[5] Rather experiments suggest the existence of inequivalent absorption sites and chain orientations.[16,21,25,31,32]

The above discussion clearly presents disagreements between theory and experiment. Two recent investigations indicate what could lead to a possible reconciliation. Maksymovych *et al.*[33] found an adatom between two methylthiol molecules with the S atoms on quasi-top positions in a combined scanning tunneling microscope (STM)/DFT study at very low coverage. Furthermore, a dynamic equilibrium between bridge site adsorption and a structure where two thiol radicals are bound to a gold adatom that has been lifted from the gold substrate was found in DFT-based molecular-dynamics (MD) calculations and confirmed in photoelectron

diffraction (PED) and GIXRD measurements.[34,35] Recent theoretical investigations involving gold adatoms have found that thiol-Au-thiol moieties adsorb on top.[36–38] Models considering surface reconstructions were first suggested by Molina and Hammer.[39] In fact, there were several indications, such as adsorption on steps,[19] surface-atom diffusion[40] and thiol-Au moieties diffusion,[41] that SAM formation and its stabilization may involve surface reconstructions.

Precise control of the self-assembly and the quality of SAM structures depend on factors such as the adsorption conditions, electrode potential, metallic surface, chain length, and stable structures.[3,4,10] For these reasons the atomistic surface structures, the nature of the $c(4\times2)$ phases, and their transformations require more investigation for an in-depth understanding.

In this work a systematic study of the $(\sqrt{3}\times\sqrt{3})R30°$ lattice and its $c(4\times2)$ superstructures of ethylthiol (ET) monolayers on Au(111) is presented, considering surface reconstructions by adatoms and vacancies. ET was used because methylthiol has less steric constrains allowing a richer diversity of phases that are not available for longer chains, while ET has a strong resemblance to long chain thiols.[42] Furthermore, ethylthiol reduces the problem that DFT/generalized gradient approximation (GGA) functionals poorly describe the van der Waals attraction. Quantum mechanics/molecular mechanics (QM/MM) calculations have shown that the van der Waals chain-chain interactions in SAM structures increase with the chain length but are negligible for $n\leq4$.[43] Thus, for ethylthiol van der Waals corrections are not necessary.

II. COMPUTATIONAL DETAILS

First-principles calculations were performed using DFT (Refs. 44 and 45) as implemented in the program VASP.[46] The exchange and correlation energy was described by the GGA functional of Perdew and Wang (PW91),[47] which at least partially recovers the van der Waals attraction.[48] The valence electron wave function was expanded in a plane-wave basis set up to a kinetic-energy cutoff of 450 eV. The projector augmented-wave (PAW) method[49,50] was used to obtain the all-electron wave function within the frozen-core approximation. Both the $(\sqrt{3}\times\sqrt{3})R30°$ lattice and its $c(4\times2)$ superlattice have been described using a $(2\sqrt{3}\times3)$ unit cell, which is the primitive cell of $c(4\times2)$, and contains four molecules and 12 gold atoms per layer. This selection allows direct comparison of the computed energies. The surface was modeled by a three-dimensional (3D) periodic supercell, consisting of a slab of four layers of gold atoms and ten layers of vacuum to avoid spurious self-interactions. The two bottom gold layers were fixed in bulk positions at the theoretical lattice constant $a=4.17$ Å. Test calculations with thicker slabs showed that the above slab gives converged adsorption energies. The Brillouin-zone integrations were performed over a $8\times8\times1$ Monkhorst-Pack grid[51] (32 k points) not including the Γ point. The first-order Methfessel-Paxton electron smearing scheme with $\sigma=0.2$ eV keeps the entropic contribution to the energy below 0.1 meV per atom, providing accurate structure optimization. All the structures were optimized until the convergence criterion of 0.01 eV/Å as maximum residual force component was reached. Our energies are converged to within ±5 meV. STM images were simulated in the Tersoff-Hamann approach[52] for different bias voltages (V_s).

The adsorption energies (E_{ads}) per molecule were calculated as

$$E_{\mathrm{ads}}=[E_{\mathrm{mol+slab}}-E_{\mathrm{slab}}-4E_{\mathrm{mol}}-(n_a-n_v)E_{\mathrm{bulk}}]/4,$$

where $E_{\mathrm{mol+slab}}$ is the total energy of the SAM structure with four molecules on the $(2\sqrt{3}\times3)$ unit cell, E_{slab} is the total energy of the clean unreconstructed slab, and E_{mol} is the energy of an isolated ethylthiol radical (CH_3-CH_2-S) calculated in a 20 Å cubic cell using only the Γ point and spin-polarized wave functions. For n_a adatoms (n_v vacancies) the energy of bulk gold atoms, E_{bulk}, is added (subtracted).

Surface energies (E_{surf}) were calculated to evaluate the energy required to create the SAM structure from bulk gold and disulfide molecules as follows:

$$E_{\mathrm{surf}}=(E_{\mathrm{mol+slab}}-2E_{\mathrm{dimer}}-n_tE_{\mathrm{bulk}}-E_{\mathrm{back}})/A.$$

Here E_{dimer} is the energy of an ethylthiol dimer (CH_3-CH_2-S-S-CH_2-CH_3) calculated in a 20 Å cubic cell using only the Γ point, n_t is the total number of gold atoms, and A is the area of the unit cell, 0.91 nm^2. E_{back} is the surface energy of the back side of the slab, calculated from the energy of the clean slab fixed in bulk position, which has two such surfaces: $E_{\mathrm{back}}=(E_{\mathrm{fixed}}-48E_{\mathrm{bulk}})/2$.

III. RESULTS AND DISCUSSION

Our search for the most stable alkylthiol/Au(111) SAM structure consists of two parts corresponding to the $(\sqrt{3}\times\sqrt{3})R30°$ and $c(2\times4)$ lattices. For the $(\sqrt{3}\times\sqrt{3})R30°$ lattice we have attempted to cover all possible structures including adatom and vacancy reconstructions consistent with the symmetry and 1/3 coverage. This requires that all molecules are on equivalent binding sites. Furthermore, only a single adatom or surface vacancy (corresponding to 1/3 monolayer) is compatible with the symmetry. For each of the three $(\sqrt{3}\times\sqrt{3})R30°$ gold surfaces (clean, with one adatom or one vacancy), the most favorable thiol adsorption site and molecule orientation was found by systematically searching the translational and orientational potential-energy surfaces (PES).[53] Figures 1(a)–1(c) show the lowest-energy fully optimized structures resulting from the minima on the respective PES.

On the clean Au(111) surface, the ethylthiol molecule is adsorbed with the sulfur atom in a bridge-like position, slightly displaced toward the fcc hollow, forming two Au-S bonds of 2.49 Å [Fig. 1(a)]. The alkyl chain is tilted by 22° in the direction of the hcp hollow. This result agrees with previous DFT studies[21,22,26–29] and was mainly included as reference structure for comparison.

The honeycomb-like gold surface reconstruction results from the formation of a 1/3 vacancy coverage in the $(\sqrt{3}\times\sqrt{3})R30°$ lattice. On this surface, the thiol molecules also adsorb in a bridge-like position on the edge of the honeycomb structure, forming two Au-S bonds of 2.42 Å, and

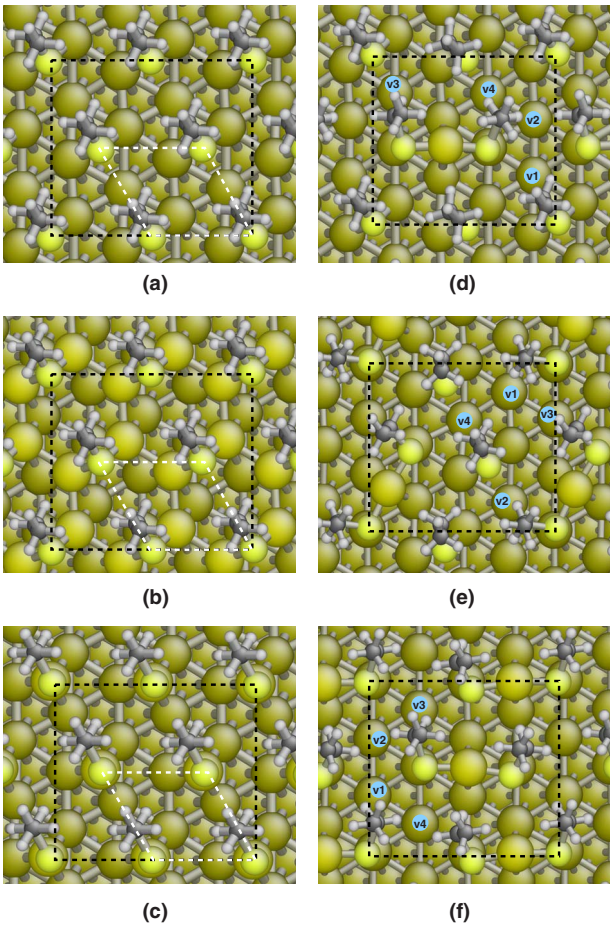

FIG. 1. (Color online) Top view of the most stable structures: (a) unreconstructed, (b) honeycomb, (c) on top, (d) and (e) single ET-Au-ET moiety, and (f) two ET-Au-ET moieties. The $(\sqrt{3}\times\sqrt{3})R30°$ and $(2\sqrt{3}\times 3)$ unit cells are highlighted by white and black dotted lines, respectively.

have a tilt angle of 27°. The adsorption energy is −1.94 eV, as compared to −1.80 eV on the clean Au(111) surface (Table I). The 1/3 monolayer of vacancies stabilizes the thiol SAM by 0.14 eV. This indicates that the thiol-gold bonds on the honeycomb reconstructed slab are considerably stronger than on a clean gold surface. However, formation of the honeycomb structure from a clean gold surface would be unfavorable by 0.65 eV. This stabilization of the SAM including vacancies is also seen in the lower surface energy of 2.67 eV/nm^2 as compared to 3.30 eV/nm^2 for the reference structure.

On the surface with 1/3 monolayer of gold adatoms, the thiol molecules adsorb on top of the adatom, forming a single Au-S bond of 2.28 Å, nearly parallel to the surface normal [Fig. 1(c)]. The adatom sits in an fcc hollow and the alkyl chain is tilted by 40°. The adsorption site on top of an adatom had been suggested previously[39,54] and may agree with the results of the diffraction studies;[55] however, the adsorption energy of only −1.50 eV and the high surface energy of 4.63 eV/nm^2 indicate that this is an unfavorable structure, considerably less stable than the reference structure.

TABLE I. Adsorption energy per molecule (E_{ads}) and surface energy (E_{surf}) for ethylthiol SAM structures.

Geometry[a]	Vacancies	E_{ads} (eV)	E_{surf} (eV/nm^2)
a	—	−1.80	3.30
b	—	−1.94	2.67
c	—	−1.50	4.63
d	—	−1.87	3.00
d	v1	−1.86	3.03
d	v2	−1.79	3.33
d	v3	−1.87	2.98
d	v4	−1.89	2.90
e	—	−1.87	2.99
e	v1	−1.80	3.31
e	v2	−1.88	2.96
e	v3	−1.81	3.26
e	v4	−1.92	2.78
f	—	−1.99	2.44
f	v1	−1.94	2.66
f	v2	−1.92	2.76
f	v3	−1.94	2.67
f	v4	−1.92	2.77
f	v1, v2	−1.91	2.83
f	v1, v3	−1.90	2.87
f	v1, v4	−1.90	2.85
f	v2, v3	−1.89	2.92
f	v2, v4	−1.85	3.07
f	v3, v4	−1.90	2.85

[a]Letters refer to subparts of Fig. 1.

A $c(4\times 2)$ structure corresponds to up to four inequivalent adsorption sites for thiol molecules on the $(2\sqrt{3}\times 3)$ primitive unit cell. We have considered up to two adatoms and vacancies. Under these circumstances the high number of degrees of freedom makes a comprehensive search of the PES impractical. As an alternative approach, we have assumed that the $c(4\times 2)$ structures may be derived from the $(\sqrt{3}\times\sqrt{3})R30°$ structure by adding adatoms or vacancies. This assumption was conceived by the observation of phase transitions between the $(\sqrt{3}\times\sqrt{3})R30°$ and the $c(4\times 2)$ structures in STM studies[18,19] and other experimental findings.[33] The starting structures have been derived by placing gold atoms between pairs of thiol molecules forming ET-Au-ET moieties. Optimization of these structures resulted in substantial movement of the molecules and adatoms across the surface, but the ET-Au-ET moieties were preserved. In the final structures, the thiol molecules are bound on top of gold surface atoms forming a nearly vertical bond of 2.52 Å. The adatoms linking two thiol molecules via Au-S bonds of 2.33 Å are in a bridge position above the midpoint of two gold atoms of the surface (Fig. 2). Both Au-Au distances are 2.96 Å.

For the case of a single adatom two orientations of the ET-Au-ET moiety were found to be favorable [see Figs. 1(d)

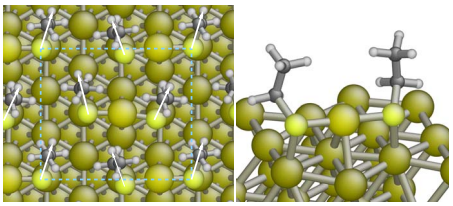

FIG. 2. (Color online) Top view of the most stable SAM structure with two ET-Au-ET moieties (left). Precession angles are indicated by white arrows. Perspective view of an adatom moiety (right).

and 1(e)], while two adatoms gave the structure shown in Fig. 1(f). Alternative starting points resulted in structures with considerably higher energies and are not included here. Comparing the surface energies and adsorption energies for these structures in Table I, it can be seen that adatoms stabilize the SAM. The adsorption energy per molecule is −1.87 eV in both structures with one adatom, indicating 0.07 eV stronger binding than on the clean surface. The surface energies are 0.3 $\mathrm{eV/nm^2}$ lower. In case of two adatoms, the adsorption energy is −1.99 eV and the surface energy is only 2.44 $\mathrm{eV/nm^2}$. This is the most stable of our SAM structures.[56]

Each of the $(2\sqrt{3}\times 3)$ adatom structures has four surface gold atoms that are not directly involved in binding the adsorption layer and hence may form a surface vacancy. The positions are numbered from 1 to 4 in Figs. 1(d)–1(f). Removal of these gold atoms resulted only in minor relaxations. Therefore the corresponding structures are not shown. The adsorption energies and surface energies are summarized in Table I. In most cases, vacancies destabilize the structures with ET-Au-ET moieties. However, six of the eight structures with one vacancy and one adatom and all of the structures with one or two vacancies and two adatoms are more stable than the reference structure. Hence simultaneous formation of ET-Au-ET moieties and vacancies is exothermic. This was also suggested by the irreversibility of such processes in DFT/MD simulations.[34,35] Structures with vacancies in different positions are almost isoenergetic. This may indicate a high thermal mobility of the vacancies. For instance, the structures with two adatoms and two vacancies differ by less than 0.1 $\mathrm{eV/nm^2}$ (excluding the unfavorable combination of v2 and v4).

A careful analysis of the structures and energies listed in Table I suggests the stepwise stabilization mechanism, illustrated in Fig. 3, which transforms the α phase [reference structure, Fig. 1(a)] into the lowest-energy structure with two ET-Au-ET moieties [Fig. 1(f)]. The dense SAM on an unreconstructed gold surface [Fig. 1(a)] may stabilize by formation of ET-Au-ET moieties+vacancies resulting in one of the structures corresponding to Fig. 1(d) with a vacancy in position v1, v3, or v4. In the next step, the structure shown in Fig. 1(f) with two ET-Au-ET moieties and a combination of two vacancies (excluding v2+v4) is formed. Simultaneous formation of adatoms and vacancies is a local process conserving the composition of the unit cell and hence may occur rapidly. However, the structures with two adatoms and two vacancies may further stabilize by reducing the number of

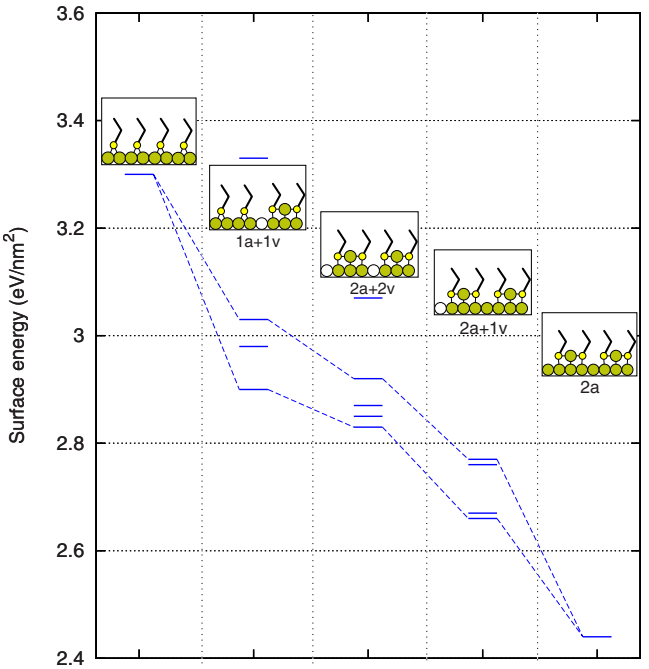

FIG. 3. (Color online) Scheme illustrating the stepwise stabilization mechanism transforming the initial $(\sqrt{3}\times\sqrt{3})R30°$ into $c(4\times 2)$ structures. Doted lines indicate the highest and lowest stabilization. Big filled circles are gold atoms, big open circles are gold vacancies, and small circles represent the sulfur headgroup. Molecules are adsorbed on bridge or on top as ET-Au-ET adatom moieties.

vacancies to one and finally to zero vacancy per unit cell. This requires diffusion of vacancies to the boundary of the dense domains, where they may form vacancy islands. Decreasing the vacancy density in the structure with two adatoms per unit cell [Fig. 1(f)] from 1/6 to 1/12 monolayer and finally to 0 stabilizes the SAM by ∼0.1–0.3 $\mathrm{eV/nm^2}$ and 0.2–0.3 $\mathrm{eV/nm^2}$, respectively.

The structures in Fig. 1(e) with vacancies v2, v3, and v4 are also more stable than the reference structure. However, the different orientation of the ET-Au-ET moiety in the unit cell does not allow formation of a second moiety without major rearrangement and hence they were not included in Fig. 3.

The SAM structure with two ET-Au-ET moieties shown in Fig. 2 is the most stable among all the structures studied, with a surface energy of 0.86 $\mathrm{eV/nm^2}$ below that of the SAM on a clean Au(111). The stabilization of the SAM due to adatoms and the formation of ET-Au-ET moieties binding in on-top position indeed reconcile the binding site controversy. The sulfur atoms are not on perfect top position but rather slightly off by 0.3 or 0.5 Å with respect to the exact top site. These deviations are in agreement with the ∼0.5 Å maximum lateral movement as suggested by experiments.[25,32] The calculated chain tilt angle is 34° in reasonable to good agreement with the experimental values of 28°,[1] 34°,[25] and 35° ± 10°.[35] Furthermore, the arrangement of precession angles of the hydrocarbon chains represented by white arrows in the Fig. 2 (left panel) has a similar configuration as proposed by Camillone *et al.*[31]

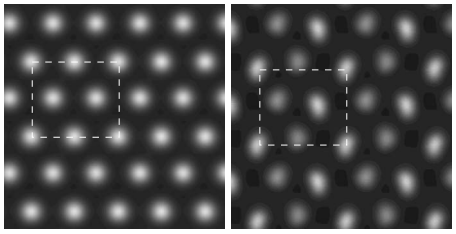

FIG. 4. Simulated STM images for the unreconstructed structure (left) and the most stable structure with two adatoms (right). Bias voltage V_s=0.4 V. The $(2\sqrt{3}\times 3)$ unit cell is highlighted by dashed lines.

The differences between the α phase and the $c(4\times 2)$ phases can be explained as a surface reconstruction. While for the α phase the molecules bind in bridge position to an unreconstructed flat Au(111) surface resulting in a perfect $(\sqrt{3}\times\sqrt{3})R30°$ hexagonal lattice, in $c(4\times 2)$ phases the molecules are coupled by adatoms in thiol-Au-thiol pairs that bind in top position and stabilize the SAM. The height of the molecules above the gold surface differs for the two structures. The sulfur atoms in the reference structure and our most stable structure are at 2.02 and 2.61 Å above the gold surface (defined by the average height of the top layer), respectively. Diffraction experiments gave heights of 2.42 ± 0.03,[23] 2.50 ± 0.05,[24] and 2.44 Å.[25] The experimental values are in between the results from our calculations, as experimental SAMs are composed of a variable mixture of phases.

Figure 4 shows the calculated STM images with V_s =0.4 V for the unreconstructed structure [Fig. 1(a)] and the most stable structure with two ET-Au-ET moieties [Fig. 1(f)]. STM images show changes in adsorption sites and molecular orientations as intensity variation.[57] The STM image of the unreconstructed structure necessarily gives the hexagonal pattern of the α phase as all thiols are in equivalent positions. The most stable structure displays a clearly visible zigzag pattern that resembles the intensity modulation reported in many molecular resolution STM experiments. The zigzag is characteristic of the δ phase, which is the most frequently observed phase.[17] The intensity variation in Fig. 4 (right panel) is due to slight differences in the positions of the sulfur atoms and the tilting and precession angles of the alkyl chain, as shown in Fig. 2.

IV. CONCLUSIONS

The energetically most stable SAM structure is characterized by a reconstruction due to two adatoms per $(2\sqrt{3}\times 3)$ unit cell, corresponding to 1/6 of a monolayer. The thiols are organized in ET-Au-ET moieties forming one bond to an adatom and one bond to surface gold atoms. The sulfur atom is approximately in top position, contrary to SAM structures without adatoms (where thiols bind on bridge position). Therefore, this most stable structure reconciles the binding site controversy. It also agrees with other geometrical results derived from diffraction experiments. Furthermore, this structure has a $c(4\times 2)$ superlattice and the simulated STM image shows the zigzag intensity modulation characteristic for the δ phase, which is one of the most frequently observed patterns seen in STM experiments.

The stabilizing ET-Au-ET moieties are formed from thiols in bridge positions and adatoms taken from the top gold layer generating local single-atom vacancies. The SAM may then stabilize further by diffusion of the vacancies to the domain boundaries. This may explain the nearby formation of vacancy islands, a characteristic phenomenon observed during the condensation of the high-density phases. This stepwise stabilization mechanism transforms the unreconstructed SAM structure with $(\sqrt{3}\times\sqrt{3})R30°$ lattice into the most stable structure with $c(4\times 2)$ superlattice. The present study highlights important intermediate structures of this process; however, the detailed dynamics will require further investigation.

ACKNOWLEDGMENTS

This work was done in the framework of the International Max-Planck Research School for Surface and Interface Engineering in Advanced Materials (IMPRS-SurMat). We thank Michael Rohwerder for stimulating discussions.

*Present address: WACKER SCHOTT Solar GmbH, Jena, Germany.
†biedermann@mpie.de

[1] J. Love, L. Estroff, J. Kriebel, R. Nuzzo, and G. Whitesides, Chem. Rev. (Washington, D.C.) **105**, 1103 (2005).
[2] G. G. Baralia, A. Pallandre, B. Nysten, and A. M. Jonas, Nanotechnology **17**, 1160 (2006).
[3] D. L. Allara, Biosens. Bioelectron. **10**, 771 (1995).
[4] H. Akkerman, A. Kronemeijer, P. van Hal, D. de Leeuw, P. Blom, and B. de Boer, Small **4**, 100 (2008).
[5] C. Vericat, M. E. Vela, G. A. Benitez, J. A. M. Gago, X. Torrelles, and R. C. Salvarezza, J. Phys.: Condens. Matter **18**, R867 (2006).
[6] G. E. Poirier and E. D. Pylant, Science **272**, 1145 (1996).
[7] F. Schreiber, Prog. Surf. Sci. **65**, 151 (2000).
[8] M. Dishner, J. Hemminger, and F. Feher, Langmuir **13**, 2318 (1997).
[9] G. Poirier, Langmuir **13**, 2019 (1997).
[10] M. Rohwerder, K. de Weldige, and M. Stratmann, J. Solid State Electrochem. **2**, 88 (1998).
[11] O. Cavalleri, A. Hirstein, and K. Kern, Surf. Sci. **340**, L960 (1995).
[12] X. Torrelles, E. Barrena, C. Munuera, J. Rius, S. Ferrer, and C. Ocal, Langmuir **20**, 9396 (2004).
[13] P. Fenter, P. Eisenberger, and K. S. Liang, Phys. Rev. Lett. **70**, 2447 (1993).
[14] I. Touzov and C. B. Gorman, J. Phys. Chem. B **101**, 5263 (1997).

[15] E. Paradis and P. Rowntree, J. Electroanal. Chem. **550-551**, 175 (2003).
[16] R. G. Nuzzo, E. M. Korenic, and L. H. Dubois, J. Chem. Phys. **93**, 767 (1990).
[17] B. Lüssem, L. Müller-Meskamp, S. Karthäuser, and R. Waser, Langmuir **21**, 5256 (2005).
[18] F. Terán Arce, M. E. Vela, R. C. Salvarezza, and A. J. Arvia, J. Chem. Phys. **109**, 5703 (1998).
[19] C. Vericat, G. Andreasen, M. E. Vela, H. Martin, and R. C. Salvarezza, J. Chem. Phys. **115**, 6672 (2001).
[20] A. Ulman, Chem. Rev. (Washington, D.C.) **96**, 1533 (1996).
[21] M. C. Vargas, P. Giannozzi, A. Selloni, and G. Scoles, J. Phys. Chem. B **105**, 9509 (2001).
[22] Y. Yourdshahyan and A. M. Rappe, J. Chem. Phys. **117**, 825 (2002).
[23] H. Kondoh, M. Iwasaki, T. Shimada, K. Amemiya, T. Yokoyama, T. Ohta, M. Shimomura, and S. Kono, Phys. Rev. Lett. **90**, 066102 (2003).
[24] M. Roper, M. Skegg, C. Fisher, J. Lee, V. Dhanak, D. Woodruff, and R. G. Jones, Chem. Phys. Lett. **389**, 87 (2004).
[25] X. Torrelles *et al.*, J. Phys. Chem. B **110**, 5586 (2006).
[26] H. Grönbeck, A. Curioni, and W. Andreoni, J. Am. Chem. Soc. **122**, 3839 (2000).
[27] Y. Akinaga, T. Nakijima, and K. Hirao, J. Chem. Phys. **114**, 8555 (2001).
[28] T. Hayashi, Y. Morikawa, and H. Nozoye, J. Chem. Phys. **114**, 7615 (2001).
[29] J. Gottschalck and B. Hammer, J. Chem. Phys. **116**, 784 (2002).
[30] Y. Morikawa, T. Hayashi, C. C. Liew, and H. Nozoye, Surf. Sci. **507-510**, 46 (2002).
[31] N. Camillone III, C. E. D. Chidsey, G. yu Liu, and G. Scoles, J. Chem. Phys. **98**, 3503 (1993).
[32] P. Fenter, F. Schreiber, L. Berman, G. Scoles, P. Eisenberger, and M. J. Bedzyk, Surf. Sci. **412-413**, 213 (1998).
[33] P. Maksymovych, D. C. Sorescu, and J. T. Yates, Phys. Rev. Lett. **97**, 146103 (2006).
[34] R. Mazzarello, A. Cossaro, A. Verdini, R. Rousseau, L. Casalis, M. F. Danisman, L. Floreano, S. Scandolo, A. Morgante, and G. Scoles, Phys. Rev. Lett. **98**, 016102 (2007).
[35] A. Cossaro *et al.*, Science **321**, 943 (2008).
[36] A. Nagoya and Y. Morikawa, J. Phys.: Condens. Matter **19**, 365245 (2007).
[37] J.-g. Wang and A. Selloni, J. Phys. Chem. C **111**, 12149 (2007).
[38] H. Grönbeck, H. Häkkinen, and R. L. Whetten, J. Phys. Chem. C **112**, 15940 (2008).
[39] L. M. Molina and B. Hammer, Chem. Phys. Lett. **360**, 264 (2002).
[40] T. Ohgi, H. Y. Sheng, Z. C. Dong, and H. Nejoh, Surf. Sci. **442**, 277 (1999).
[41] S. J. Stranick, A. N. Parikh, D. L. Allara, and P. S. Weiss, J. Phys. Chem. **98**, 11136 (1994).
[42] S. Franzen, Chem. Phys. Lett. **381**, 315 (2003).
[43] D. Fischer, A. Curioni, and W. Andreoni, Langmuir **19**, 3567 (2003).
[44] P. Hohenberg and W. Kohn, Phys. Rev. **136**, B864 (1964).
[45] W. Kohn and L. J. Sham, Phys. Rev. **140**, A1133 (1965).
[46] G. Kresse and J. Furthmüller, Phys. Rev. B **54**, 11169 (1996).
[47] J. P. Perdew and Y. Wang, Phys. Rev. B **45**, 13244 (1992).
[48] S. Tsuzuki and H. P. Luthi, J. Chem. Phys. **114**, 3949 (2001).
[49] P. E. Blöchl, Phys. Rev. B **50**, 17953 (1994).
[50] G. Kresse and D. Joubert, Phys. Rev. B **59**, 1758 (1999).
[51] H. J. Monkhorst and J. D. Pack, Phys. Rev. B **13**, 5188 (1976).
[52] J. Tersoff and D. R. Hamann, Phys. Rev. B **31**, 805 (1985).
[53] E. Torres, A. T. Blumenau, and P. U. Biedermann (unpublished).
[54] F. P. Cometto, P. Paredes-Olivera, V. A. Macagno, and E. M. Patrito, J. Phys. Chem. B **109**, 21737 (2005).
[55] M. Yu, N. Bovet, C. J. Satterley, S. Bengió, K. R. J. Lovelock, P. K. Milligan, R. G. Jones, D. P. Woodruff, and V. Dhanak, Phys. Rev. Lett. **97**, 166102 (2006).
[56] The above structures were presented at the 6th Congress of the International Society for Theoretical Chemical Physics, Vancouver, Canada, 2008.
[57] C. Zeng, B. Li, B. Wang, H. Wang, K. Wang, J. Yang, J. G. Hou, and Q. Zhu, J. Chem. Phys. **117**, 851 (2002).